Inorganic Chemistry

Article

pubs.acs.org/IC

New Al-MOFs Based on Sulfonyldibenzoate Ions: A Rare Example of Intralayer Porosity

Nele Reimer,[†] Helge Reinsch,[‡] A. Ken Inge,[†] and Norbert Stock*,[†]

[†]Institut für Anorganische Chemie, Christian-Albrechts-Universität zu Kiel, Max-Eyth-Strasse 2, D-24118 Kiel, Germany

[‡]INGAP Centre of Research-Based Innovation, Department of Chemistry, University of Oslo, Sem Saerlandsvei 26, N-0315 Oslo, Norway

Supporting Information

ABSTRACT: A new sulfone-functionalized metal−organic framework [Al(OH)(SDBA)]·0.25DMF, denoted CAU-11, was synthesized using a V-shaped linker molecule 4,4′-sulfonyldibenzoic acid (H_2SDBA). The crystal structure was solved from synchrotron X-ray powder diffraction data. Chains of trans corner-sharing AlO_6 octahedra are interconnected by the carboxylate groups to form layers (ABAB stacking). Within the layers, hydrophobic lozenge-shaped pores with a diameter of 6.4 × 7.1 Å^2 are present inducing permanent porosity (a_{BET} = 350 m^2 g^{-1} and V_{micro} = 0.17 cm^3 g^{-1}). With the application of HT-methods (HT = high throughput), the isoreticular carboxylate functionalized compound [Al(OH)(H_2DPSTC)]·0.5H_2O (CAU-11-COOH) was synthesized using the linker molecule 3,3′,4,4′-diphenylsulfonetetracarboxylic dianhydride (DPSDA), which hydrolyzes under the reaction conditions. Due to the additional noncoordinating carboxylic acid groups the pores are hydrophilic. Changing the molar ratio of Al^{3+} to linker lead to the discovery of a second new compound [Al_2(OH)$_2$(DPSTC)(H_2O)$_2$]·0.5H_2O (CAU-12). In CAU-12 the linker molecule is fully deprotonated which leads to different connectivity compared to the structure of CAU-11-COOH. Thermal activation of CAU-12 leads to dehydration and transformation of the structure to [Al_2(OH)$_2$(DPSTC)]·$n H_2O$ (CAU-12-dehy). Coordinated water molecules were removed, and the coordination site is replaced by the previously noncoordinating O atom of the adjacent carboxylate group. The SO_2-groups point into the pores resulting in a highly hydrophobic three-dimensional framework. The compounds exhibit high thermal stability in air at least up to 420 °C. Synthesis of CAU-11 can be easily scaled up in very high yields (98%).

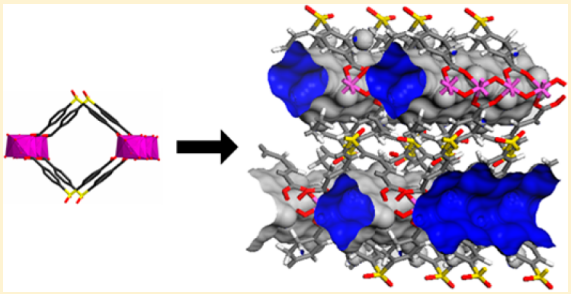

INTRODUCTION

In the field of porous materials, metal−organic frameworks (MOFs) have drawn much attention during the last two decades.[1−3] This is probably due to their modular assembly and their potential applications in the fields of gas storage and separation, catalysis, or drug delivery.[4−6] MOFs are built up from inorganic and organic building units. By variation of one of the building units by a chemically different but topologically equivalent unit, it is possible to modulate the properties of a compound. This approach is called isoreticular chemistry.[7] The synthesis of isoreticular compounds is not always easily accomplished since changing one component in the synthesis mixture often necessitates optimization of the reaction conditions of the desired compound. The reaction product of a solvothermal synthesis depends on many different reaction parameters, and systematic studies are therefore of great advantage. High-throughput (HT) methods have shown to be an important and efficient tool to accomplish this task.[8−10] We focused our work on MOFs based on Al^{3+} ions since these materials are known for their excellent thermal and chemical stability.[11,12] This makes them suitable for postsynthetic modification reactions and renders them as potential candidates for storage and separation or heat transformation processes.[4,13−15] In addition, aluminum is nontoxic, and the inorganic starting materials are in general inexpensive, which makes these compounds interesting for industrial applications.[16] Al-MIL-53 (MIL = Materiaux de l'Institute Lavoisier) is a very well-known Al-MOF that contains terephthalate ions.[17] Its structure is based on chains of trans corner-sharing AlO_6 octahedra which are interconnected by the carboxylate groups of the linker molecules, to build up a three-dimensional framework with lozenge-shaped pores. The inorganic building unit of MIL-53 is very common in other Al-MOFs based on linear linker molecules.[18−22] During the past two years we investigated the influence of the linker shape on the formation of the inorganic building unit and the resulting MOF structure.[20,23−27] V-shaped linkers were chosen for these studies (Figure 1).

The use of (functionalized) isophthalic acid (Figure 1, **1**) led to the porous compound [Al(OH)(*m*-BDC)]·solvent (CAU-10).[25] Its structure is built of helices of cis corner-sharing AlO_6 octahedra, which are interconnected by the carboxylate groups of the linker molecule. Attempts to increase the pore size of

Received: September 16, 2014
Published: December 24, 2014

DOI: 10.1021/ic502242j
Inorg. Chem. 2015, 54, 492−501

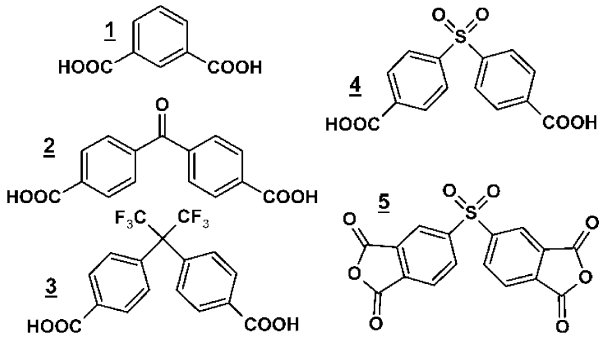

Figure 1. V-shaped linker molecules used for the synthesis of MOFs: Isophthalic acid (*m*-H_2BDC) (**1**), 4,4′-benzophenonedicarboxylic acid (**2**), 4,4′-(hexafluoroisopropylidene)bis(benzoic acid) (**3**), 4,4′-sulfonyldibenzoic acid (H_2SDBA) (**4**), and 3,3′,4,4′-diphenylsulfontetracarboxylic dianhydride (DPSDA) (**5**).

CAU-10 by replacing the isophthalic acid with the extended but more flexible linker 4,4′-benzophenonedicarboxylic acid (H_2BPDC, Figure 1, **2**) resulted in a new compound [Al(OH)(BPDC)]·solvent (CAU-8), which contains MIL-53 type inorganic building units.[26] Other larger V-shaped linkers have only sparsely been used in the synthesis of MOFs in combination with trivalent cations. Thus, only a few examples based on 4,4′-(hexafluoroisopropylidene)bis(benzoic acid) (Figure 1, **3**) and rare-earth metals[28,29] as well as one compound containing In^{3+} ions[30] are known. The geometry of 4,4′-sulfonyldibenzoic acid (H_2SDBA) is also very similar to that of H_2BPDC. This linker has been more extensively used (Supporting Information Table S1), but its reactions with trivalent cations have only resulted in three nonporous compounds so far based on neodymium, ytterbium, and erbium.[31] Several other compounds are known on the basis of mono- or bivalent cations with one-, two-, or three-dimensional structures. Among these, only a few of them, $[Cs_2Pb_2(SDBA)_3(DMF)]\cdot DMF$,[32] $[Ca(SDBA)]\cdot 0.45H_2O$,[33] and [Ca(SDBA)],[34] as well as $[Zn_3(OH)_2(SDBA)_2]\cdot EtOH$ and $[M_3(OH)_2(SDBA)_2(EtOH)(H_2O)_3]\cdot 3.5H_2O$ (M = Mg, Ni, Co),[35] exhibit permanent porosity (Supporting Information Table S1).

In this Article we present the results of our high-throughput investigation of the systems Al^{3+}/H_2SDBA/solvent/additive and Al^{3+}/DPSDA/solvent/additive based on the V-shaped ligands 4,4′-sulfonyldibenzoic acid (H_2SDBA, Figure 1, structure 4) and 3,3′,4,4′-diphenylsulfonetetracarboxylic dianhydride (DPSDA, Figure 1, structure 5). Four new compounds were obtained and characterized in detail by X-ray powder diffraction (PXRD), vibrational spectroscopy, thermogravimetric measurements and elemental analysis as well as temperature dependent X-ray powder diffraction and sorption measurements.

EXPERIMENTAL SECTION

Chemicals. All chemicals are commercially available and were employed without further purification.

Methods. Details of the HT studies for the discovery of CAU-11, CAU-11-COOH, and CAU-12 are described in the Supporting Information. HT-experiments under conventional heating were carried out in custom-made steel-multiclaves in Teflon-lined reaction vessels.[10] HT-experiments under microwave-assisted heating were performed in glass vials which were placed in a SiC block. Reactions were carried out in a microwave reaction system Synthos3000 by Anton Paar.[12] In order to scale-up the reactions, custom-made steel autoclaves containing Teflon-inlets with a volume of 30 mL were used. The initial characterization by means of PXRD was carried out on a STOE-Stadi-P combi diffractometer (Cu Kα_1 radiation) equipped with an *xy*-stage and an image plate detector system. The synchrotron PXRD data for the structure determination and refinement of CAU-11, [Al(OH)(SDBA)], and CAU-11-COOH, $[Al(OH)(H_2DPSTC)]\cdot 0.5H_2O$, were measured at the MS-POWDER beamline (X04SA), EH1 at the Swiss Light Source, Paul Scherrer Institute, Villigen, Switzerland. The wavelength was set to 1.000 009 Å, and the pattern was recorded on a MYTHEN II detector.[36] The data for structure determination and refinement of CAU-12, $[Al_2(OH)_2(DPSTC)(H_2O)_2]\cdot 0.5H_2O$, and CAU-12-dehy, $[Al_2(OH)_2(DPSTC)]\cdot nH_2O$, were collected on a STOE-Stadi-P diffractometer (Cu Kα_1-radiation) equipped with a PSD detector.

The temperature-dependent PXRD experiments were performed in Debye−Sherrer mode on a STOE Stadi-P diffractometer (Cu Kα_1, λ = 1.5406 Å) equipped with a STOE high temperature capillary furnace. Each powder pattern was recorded in the range 3−90° (2Θ). CAU-11 was investigated in the range from 20 °C up to 660 °C in steps of 40 °C. Each measurement was collected for 20 min, and the heating rate was 5 K min^{-1}. The patterns for CAU-11-COOH were recorded in the range 20 °C up to 660 °C in steps of 40 °C. Each measurement was collected for 15 min, and the heating rate was 10 K min^{-1}. CAU-12 was studied in the range from 30 °C up to 270 °C in steps of 20 °C and from 270 °C up to 620 °C in steps of 50 °C. Each measurement was collected for 15 min, and the heating rate was 5 and 10 K min^{-1}, respectively. IR spectra were recorded on a Bruker ALPHA-FT-IR A220/D-01 spectrometer equipped with an ATR-unit. The thermogravimetric (TG) analyses were carried out using a NETSCH STA 409 CD analyzer. The samples were heated in Al_2O_3 crucibles at a rate of 4 K min^{-1} under a flow of air (25 mL min^{-1}). The contents of carbon, hydrogen, nitrogen, and sulfur were determined by elemental chemical analysis on a Eurovektor EuroEA elemental analyzer. Gas sorption experiments were performed using a BEL JAPAN INC. Belsorpmax instrument. Nitrogen and hydrogen measurements were carried out at 77 K and carbon dioxide, methane, and water vapor measurements at 298 K.

HT-Experiments. CAU-11 ([Al(OH)(SDBA)]·0.25DMF) was discovered in the system $AlCl_3\cdot 6H_2O$/H_2SDBA/H_2O/NaOH. Reactions were carried out under solvothermal reaction conditions using our custom-made HT-reactors containing 24 Teflon inlets with a maximum volume of 2 mL.[10] First the solid starting materials ($AlCl_3\cdot 6H_2O$ and H_2SDBA) were placed in the inlets, followed by the addition of H_2O and then NaOH. Six different ratios of $AlCl_3\cdot 6H_2O$ to H_2SDBA (3:1−1:3, 1 equiv corresponds to 0.06 mmol) were chosen and repeated four times, with different amounts of NaOH as additive (0−4 equiv). Details of the exact chemical and physical parameters employed in the discovery of [Al(OH)(SDBA)]·0.25DMF are listed in the Supporting Information (Table S2). For the optimization of the purity and crystallinity of the product, the following synthesis parameters were systematically varied: (1) the Al^{3+}-sources ($Al(NO_3)_3\cdot 9H_2O$, $AlCl_3\cdot 6H_2O$, $Al_2(SO_4)_3\cdot 18H_2O$, and $Al(ClO_4)_3\cdot 9H_2O$), (2) the overall concentrations (0.06−0.27 mol/L), and (3) the molar ratios of Al^{3+} to H_2SDBA (6:3−1:3 equiv). In addition the influence of additives (HCl and NaOH), the reaction temperature (120−170 °C), and the reaction time (12−36 h) was studied.

CAU-11-COOH ($[Al(OH)(H_2DPSTC)]\cdot 0.5H_2O$) was discovered in the system Al^{3+}/DPSDA/H_2O/NaOH. Reactions were carried out in analogy to the procedure described for CAU-11, but the HT-experiments were performed under microwave-assisted heating.[12] The solid starting materials were placed in glass vials with a maximum volume of 3 mL, followed by the addition of H_2O, aqueous Al^{3+} solution, and NaOH. The vials were closed with a Teflon seal and a screw cap and then placed in a SiC block, suitable for microwave heating. Details of the exact chemical and physical parameters employed for the discovery of $[Al(OH)(H_2DPSTC)]\cdot 0.5H_2O$ are listed in the Supporting Information (Table S3). For the optimization of the purity and crystallinity of the product, the following synthesis parameters were systematically varied: (1) Al^{3+} sources ($Al(NO_3)_3\cdot 9H_2O$, $AlCl_3\cdot 6H_2O$, $Al_2(SO_4)_3\cdot 18H_2O$, and $Al(ClO_4)_3\cdot 9H_2O$), (2) the

DOI: 10.1021/ic502242j
Inorg. Chem. 2015, 54, 492−501

Table 1. Summary of the Crystallographic Parameters of the Rietveld Refinements of $[Al(OH)(SDBA)]$, $[Al_2(OH)_2(DPSTC)(H_2O)_2]\cdot 0.5H_2O$, and $[Al_2(OH)_2(DPSTC)]\cdot nH_2O$, and the Parameters of $[Al(OH)(H_2DPSTC)]\cdot 0.5H_2O$ obtained from a Pawley Fit

	CAU-11 $[Al(OH)(SDBA)]$[a]	CAU-11-COOH $[Al(OH)(H_2DPSTC)]$[a]	CAU-12 $[Al_2(OH)_2(DPSTC)(H_2O)_2]\cdot 0.5H_2O$	CAU-12-dehy $[Al_2(OH)_2(DPSTC)]\cdot nH_2O$
structure determined from	powder data		powder data	powder data
λ/Å	1.000 009	1.000 009	1.5406	1.5406
formula sum	$AlC_{14}H_9O_7S$	$AlC_{16}H_{11}O_{11}S$	$Al_2C_{16}H_{15}O_{14.5}S$	$Al_2C_{16}H_{10+2n}O_{12+n}S$
Z	4	4	1	1
cryst syst	orthorhombic	orthorhombic	triclinic	triclinic
a/Å	6.6111(5)	6.6551(3)	6.6872(4)	6.3521(6)
b/Å	12.888(1)	19.9428(12)	6.6878(6)	7.1524(9)
c/Å	20.020(1)	12.9656(7)	13.6148(11)	13.7010(15)
α/deg	90	90	84.698(8)	81.841(12)
β/deg	90	90	84.705(5)	88.967(7)
γ/deg	90	90	61.126(5)	64.2526(7)
V/Å^3	1705.9(2)	1720.5(2)	530.12(8)	544.41(11)
space group	*Pnma*	$Pna2_1$	$P\bar{1}$	$P\bar{1}$
solution method	real space method, FOX[37]		structural model from the literature[38]	structural model derived from CAU-12
refinement method	least-squares Rietveld method[39]	Pawley method[39]	least-squares Rietveld method[39]	least-squares Rietveld method[39]
R_{wp}	7.7	3.3	7.6	6.1
R_{Bragg}	1.4		1.4	1.0

[a]Samples were activated prior to the PXRD measurements to remove the solvent molecules.

DOI: 10.1021/ic502242j
Inorg. Chem. 2015, 54, 492−501

overall concentration (0.067− 0.267 mol/L), and (3) the molar ratios of Al^{3+} and DPSDA (4:2−2:4 equiv). In addition the influences of reaction temperature (150−170 °C) and reaction time (3−5 h) were studied.

In the course of this systematic investigation the second phase $[Al_2(OH)_2(DPSTC)(H_2O)_2]\cdot 0.5H_2O$ (CAU-12) was discovered (Supporting Information Figure S2). Synthesis optimization was performed for CAU-12 as was for CAU-11-COOH. Details of the exact chemical and physical parameters employed for the synthesis of $[Al_2(OH)_2(DPSTC)(H_2O)_2]\cdot 0.5H_2O$ are listed in the Supporting Information (Table S4).

Optimized Reaction Conditions for [Al(OH)(SDBA)]·0.25DMF. The optimized synthesis parameters obtained from the HT-investigations were used for the synthesis scale up of CAU-11. CAU-11 is synthesized from a mixture of $AlCl_3\cdot 6H_2O$ (724 mg, 3 mmol), 4,4′-sulfonyldibenzoic acid (H_2SDBA) (268 mg, 1.2 mmol), 2 M aqueous solution of NaOH (1.8 mL, 3.6 mmol), and 18.2 mL of H_2O (no homogenization was necessary). The Teflon-liner was placed in a steel autoclave with a volume of 30 mL. The reaction was performed under conventional heating at 150 °C for 12 h, with 1 h heating up and 1 h cooling down. To remove free linker molecules as detected by IR spectroscopy, the resulting precipitate was filtered off and washed with DMF under microwave heating at 150 °C for 1 h. After being cooled to room temperature, the solid was filtered and dried in air. Yield ∼420 mg (∼98% based on H_2SDBA). Elemental analysis: N 0.82%, C 46.63%, H 2.70%, S 8.41%. Calculated values based on the molecular formula [Al(OH)(SDBA)]·0.25DMF: N 0.96%, C 48.33%, H 2.94%, S 8.74%.

Optimized Reaction Conditions for [Al(OH)(H_2DPSTC)]·0.5H_2O. CAU-11-COOH could only be obtained in the miniaturized reactors. CAU-11-COOH was synthesized in a 5 mL glass vial from a mixture of DPSDA (53.7 mg, 0.15 mmol), 1 M aqueous solution of $AlCl_3\cdot 6H_2O$ (75 μL, 0.15 mmol), and 1425 μL of H_2O (no homogenization was necessary). The reaction was carried out in a HT-microwave oven at 170 °C for 5 h. After cooling to room temperature, the precipitate was filtered off and dried in air. Yield ∼35 mg (∼50% based on DPSDA). Elemental analysis: C 43.23%, H 2.04%, S 7.46%. Calculated values based on the molecular formula $[Al(OH)(H_2DPSTC)]\cdot 0.5H_2O$: C 45.60%, H 2.88%, S 7.60%.

Optimized Reaction Conditions for $[Al_2(OH)_2(DPSTC)(H_2O)_2]\cdot 0.5H_2O$. CAU-12 was synthesized using a large excess of Al^{3+} ions in a mixture of DPSDA (17.9 mg, 0.05 mmol), 1000 μL of H_2O, and 1 M aqueous solution of $Al(NO_3)_3\cdot 9H_2O$ (500 μL, 0.5 mmol). The starting materials were placed in a 5 mL glass vial, and the reaction was carried out in a HT-microwave oven at 170 °C for 5 h. After cooling to room temperature, the precipitate was filtered off and dried in air. Upscaling of the reaction was not yet achieved. Yield ∼20 mg (∼85% based on DPSDA). Elemental analysis: C 37.32%, H 2.29%, S 5.84%. Calculated values based on the molecular formula $[Al_2(OH)_2(DPSTC)(H_2O)_2]\cdot 0.5H_2O$: C 36.72%, H 2.50%, S 6.13%.

Activation. Prior to the sorption measurements the samples were thermally activated. CAU-11 and CAU-11-COOH were heated overnight at 200 °C under vacuum ($p \leq 10^{-2}$ kPa), and CAU-12 was treated overnight at 250 °C under vacuum ($p \leq 10^{-2}$ kPa).

Structure Determination. All crystal data and the results of the refinement of [Al(OH)(SDBA)], $[Al_2(OH)_2(DPSTC)(H_2O)_2]\cdot 0.5H_2O$, and $[Al_2(OH)_2(DPSTC)]\cdot nH_2O$, as well as the results of the Pawley-fit of $[Al(OH)(H_2DPSTC)]\cdot 0.5H_2O$, are summarized in Table 1. Bond lengths are provided in the Supporting Information (Tables S5−S7). The asymmetric units of CAU-11, CAU-12, and CAU-12-dehy are shown in Supporting Information Figures S3, S4, and S5, respectively.

Crystal Structure Determination of [Al(OH)(SDBA)]. The crystal structure of CAU-11 was determined from PXRD data obtained at the MS-POWDER beamline (X04SA), EH1 at the Swiss Light Source, Paul Scherrer Institut, Villigen, Switzerland. The wavelength was set to 1.000 009 Å, and the pattern was recorded on a MYTHEN II detector.[36] The sample, activated for 2 h at 200 °C, was measured in a 0.5 mm capillary. The powder pattern was indexed and refined using TOPAS Academic.[39] The structure was solved in the space group $Pna2_1$ by real space methods using the program FOX.[37] Fenske−Hall Z matrices of an AlO_6 octahedron and an SDBA linker without the oxygen atoms of the carboxylate groups were used as input. Rietveld refinement was performed using TOPAS Academic[39] in the higher symmetry space group $Pnma$. A Z matrix was used for bond restraints and constraints.

Pawley Refinement of [Al(OH)(H_2DPSTC)]. The high-resolution powder pattern of CAU-11-COOH was obtained at the synchrotron MS-POWDER beamline (X04SA), EH1 at the Swiss Light Source, Paul Scherrer Institut, Villigen, Switzerland, with a wavelength of λ = 1.000 009 Å and a MYTHEN II detector.[36] Prior to the measurement the compound was transferred into a 0.5 mm capillary and activated for 2 h at 200 °C under vacuum. The pattern was indexed with TOPAS Academic[39] in the space group $Pna2_1$, and a Pawley refinement resulted in very similar cell parameters to CAU-11 (Table 1). The final Pawley plot is shown in Figure 2.

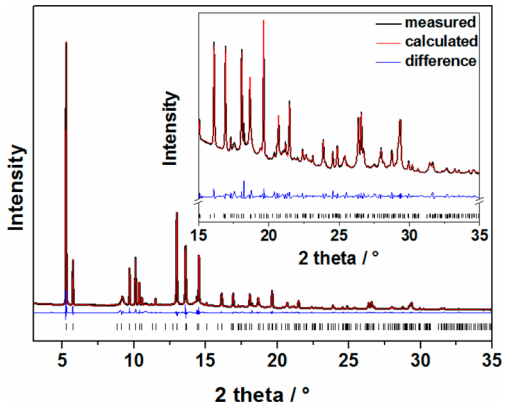

Figure 2. Pawley plot of the synchrotron high-resolution powder X-ray diffraction pattern of [Al(OH)(H_2DPSTC)] using the program TOPAS Academics V4.1.[39] The inset shows the enlarged area of 15−35° (2θ).

Attempts to determine the structure were done by constructing a suitable starting model using force-field calculations as implemented in Materials Studio.[40] The structure of CAU-11 was taken as a starting model, and the noncoordinating carboxylate groups were added. The two additional −COOH groups per linker molecule are probably statistically distributed over four different crystallographic positions (see Supporting Information for details, Figures S6−S11), and hence, the space group $Pna2_1$ was retained. Possible structures with ordered −COOH groups were optimized by force field calculations using the forcite routine (Universal force field), keeping the experimentally determined lattice parameters constant (Supporting Information Figures S8−S11). The optimized structures were used to calculate the corresponding PXRD patterns (Supporting Information Figure S7). The relative reflection intensities in the simulated PXRD patterns deviate from the ones observed in the recorded PXRD pattern. Hence we conclude that the −COOH groups are statistically distributed in the structure of CAU-11-COOH.

Crystal Structure Determination of $[Al_2(OH)_2(DPSTC)(H_2O)_2]\cdot 0.5H_2O$. A structural model for the Rietveld refinement of CAU-12 was set up using a related crystal structure as starting point for force-field calculations. Indexing of the powder pattern indicated a possible triclinic cell [a = 6.6861(19) Å, b = 6.7921(16) Å, c = 13.5998(21) Å, α = 90.196(11)°, β = 84.653(14)°, γ = 59.474(13)°] which can be considered as an expanded structure of MIL-60,[38] a vanadium pyromellitate with the composition $[V(OH)_2((O_2C)_2\text{-}C_6H_2\text{-}(CO_2)_2)]\cdot 4H_2O$ which crystallizes in the space group $P\bar{1}$. In this structure the linker molecules also bear vicinal carboxylate groups at the benzene ring. Hence a structural model for CAU-12 was constructed using Materials Studio.[40] The vanadium atoms were replaced by aluminum atoms, and the experimental cell parameters were adapted. Subsequently the C_6H_2 unit of the pyromellitate ion was

DOI: 10.1021/ic502242j
Inorg. Chem. 2015, 54, 492−501

replaced by (C_6H_3–SO_2–C_6H_3), see Supporting Information Figure S12, and the whole structure was energetically minimized by force field calculations using the forcite routine (Universal force field). In this starting model, the SO_2 groups were statistically distributed over two symmetry equivalent positions, and therefore, their occupancy was set to 0.5. The resulting structure model was refined by Rietveld methods. The aromatic benzene rings were constrained as rigid bodies while all other atoms were freely refined. Residual electron density inside the channels was located by Fourier synthesis and attributed to water molecules represented by oxygen atoms.

It is worth mentioning that an Al-based analogue of MIL-60[38] exists, denoted MIL-118,[41] but this MOF crystallizes in a monoclinic space group.

Upon thermal activation at 250 °C, substantial changes of reflection positions and relative reflection intensities were observed in the PXRD pattern. The PXRD pattern was indexed in a triclinic unit cell which is related to the one determined for CAU-12 in its conventional setting [a = 6.2694(11) Å, b = 7.1684(9) Å, c = 13.7790(15) Å, α = 81.258(5)°, β = 89.360(9)°, γ = 64.732(8)°]. On the basis of the results reported for the thermal activation of MIL-118,[41] a corresponding structural transformation was anticipated for CAU-12, and a structural model was developed. In this model hydrogen bonded carboxylate groups (Al–OH_2···O_2C–) are replaced by coordinating Al–O_2C units. After structural optimization by force-field methods using the experimentally determined lattice parameters, the derived model was used for the Rietveld refinement. Residual electron density in proximity to the CO_2 and SO_2 groups was located by Fourier synthesis and attributed to partially occupied oxygen atoms representing water molecules which are present due to physisorptive rehydration. The refinement converged to reasonable values although some reflections are not perfectly described. This could be explained by the harsh thermal treatment which might induce stress/strain in the obtained framework structure.

RESULTS AND DISCUSSION

HT-Experiments. [Al(OH)(SDBA)]·0.25DMF was discovered during the investigation of the system $AlCl_3·6H_2O$/H_2SDBA/H_2O/NaOH under solvothermal conditions. In the first experiment the amounts of $AlCl_3·6H_2O$ and H_2SDBA were varied in six steps (3:1–1:3), and the amount of NaOH as additive was varied in four steps (0–4). The different molar ratios used and the results obtained from PXRD measurements of the reaction products are shown in Figure 3, top. At low overall concentrations ($AlCl_3·6H_2O$:H_2SDBA = 1:1) only X-ray amorphous products were obtained, independent of the amount of NaOH added.

At higher overall concentrations ($AlCl_3·6H_2O$:H_2SDBA = 2:2) as well as with an excess of $AlCl_3·6H_2O$ over H_2SDBA, highly crystalline CAU-11 could be obtained with or without addition of NaOH. Reactions with an excess of linker resulted in poorly crystalline CAU-11 or CAU-11 with recrystallized linker molecules. This is also shown in Figure 3, bottom, where selected powder patterns are provided. Further HT-investigations varying the molar ratios of the reactants as well as the reaction time and temperature led to the optimized synthesis conditions. These were directly used in the synthesis scale-up employing a 30 mL reactor.

The investigation of the system Al^{3+}/DPSDA/H_2O/NaOH under microwave-assisted heating and solvothermal conditions resulted in the formation of two new compounds, [Al(OH)-(H_2DPSTC)]·0.5H_2O (CAU-11-COOH) and [Al_2(OH)$_2$-(DPSTC)(H_2O)$_2$]·0.5H_2O (CAU-12). In the first experiment the amounts of $AlCl_3·6H_2O$ with respect to DPSDA were varied in eight steps (4:2–2:4), and the amount of NaOH as additive was varied in three steps (0, 2, 4 equiv). The different molar ratios used and the results obtained from PXRD

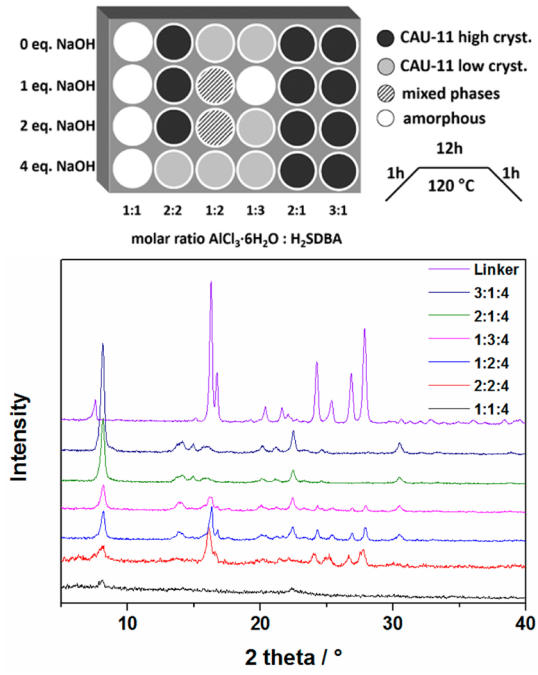

Figure 3. Top: Synthesis conditions and results of the high-throughput experiment that led to the discovery of CAU-11. Bottom: Selected powder patterns from the HT-experiment of the discovery of CAU-11. Molar ratios are given as $AlCl_3·6H_2O$:H_2DSBA:NaOH. The unit of 1 equiv corresponds to the amount of 0.06 mmol. Additional reflections in the red (2:2:4), blue (1:2:4), and magenta (1:3:4) powder patterns correspond to recrystallized linker molecules.

measurements of the reaction products are shown in Supporting Information Figure S1. CAU-11-COOH was obtained at all molar ratios without any addition of NaOH. Upon addition of NaOH a mixture of different products was found. Further HT-investigations optimizing the molar ratios of the reactants as well as the reaction time and temperature led to optimized synthesis conditions. Phase pure samples of highly crystalline CAU-12 were obtained while studying the influence of the overall concentration in the absence of NaOH as an additive (Supporting Information Figure S2). The overall concentration was varied, and different molar ratios of $AlCl_3·6H_2O$ to DPSDA, always with an excess of $AlCl_3·6H_2O$ (2:1 up to 10:1 and 3:2 up to 10:2; 1equiv = 0.05 mmol), were used. Pure CAU-12 was obtained only for the molar ratios 6:1, 5:2, and 6:2 of $AlCl_3·6H_2O$ to DPSDA. The other ratios resulted in mixtures of CAU-11-COOH and CAU-12 or pure CAU-11-COOH. Further HT-investigations optimizing the molar ratios of the reactants as well as the reaction time and temperature and the Al^{3+} source led to the optimized synthesis conditions.

Structure Description of [Al(OH)(SDBA)]. CAU-11 crystallizes as microsized particles (SEM micrograph, Supporting Information Figure S13). Hence, the structure was solved and refined from synchrotron PXRD data. The final Rietveld plot is shown in Figure 4. The structure of CAU-11 is built up from chains of trans corner-sharing AlO_6 octahedra (Figure 5, left). As observed in many other Al-MOFs, μ-OH groups are bridging adjacent Al^{3+} ions. The Al–O distances range from 1.85(4) to 1.97(2) Å, which is in good agreement with the values for recently published Al-MOFs based on the same inorganic building unit.[20,26] The chains are interconnected along the a-axis via the carboxylate groups of the linker molecules to form layers with lozenge-shaped pores (Figure 5,

DOI: 10.1021/ic502242j
Inorg. Chem. 2015, 54, 492–501

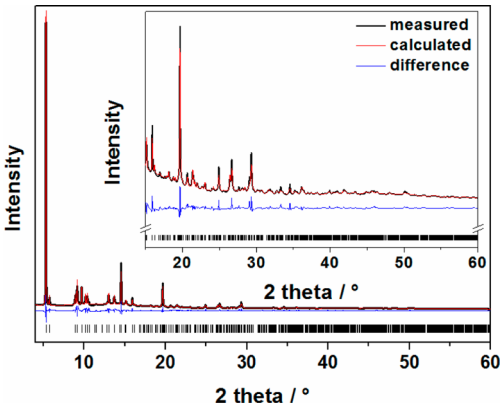

Figure 4. Final Rietveld plot of the structure refinement of [Al(OH)(SDBA)] (CAU-11). The observed powder pattern is shown in black, the calculated one is shown as an overlay in red, and the difference plot is shown in blue. The ticks mark the allowed Bragg peak positions. The inset shows the enlarged area of 15−60° (2θ).

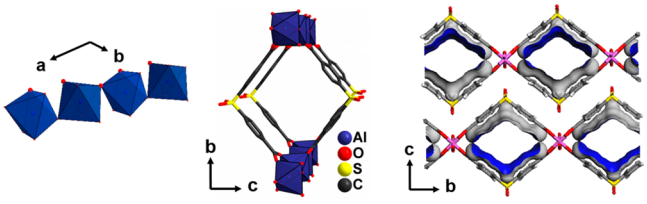

Figure 5. Structure of [Al(OH)(SDBA)]. Left: Inorganic building unit, chains of trans corner-sharing AlO_6 octahedra. Middle: Lozenge-shaped pore-channel built up by two Al−O-chains interconnected by the linker molecules. Right: Connolly surface modeled with Materials Studio.[40]

middle). These layers are stacked along the *c*-axis in an ABAB-fashion to form a layered structure (Figure 5, right) and further interact through weak hydrogen bonds (Supporting Information Figure S14). The sulfone groups do not point into the pore, but toward neighboring inorganic chains, suggesting a hydrophobic inner-pore surface. The bridging μ-OH groups are aligned along the *c*-axis pointing toward the SO_2 groups (O···O = 2.84 Å). The crystal structure of CAU-11 exhibits some relationship to [In(OH)($C_{17}H_8F_6O_4$)],[30] a material synthesized with 4,4′-(hexafluoroisopropylidene)bis(benzoic acid) as a V-shaped linker. The structure of [In(OH)($C_{17}H_8F_6O_4$)] also contains lozenge-shaped channels running through layers consisting of trans corner-sharing octahedra. However, the layers in the two structures have different topologies. The topology of CAU-11 can be described by a square lattice (4^4 net), while the net of [In(OH)($C_{17}H_8F_6O_4$)] cannot be flattened in a plane without crossing edges (Supporting Information Figure S15). The layers in [In(OH)($C_{17}H_8F_6O_4$)] exhibit ABCD type stacking.

Structure Description of $[Al_2(OH)_2(DPSTC)(H_2O)_2]\cdot 0.5H_2O$. The structure of CAU-12 was solved and refined from laboratory PXRD data. On the basis of the structure of MIL-60,[38] the structure model for CAU-12 was generated by force-field calculations using the program Materials Studio.[40] The final Rietveld plot is shown in Figure 6.

The structure of CAU-12 is related to the one of MIL-60 and MIL-118A and consists of infinite chains of two types of trans corner-sharing AlO_6 octahedra which are connected in an alternating fashion. In the first type of AlO_6 octahedra, four

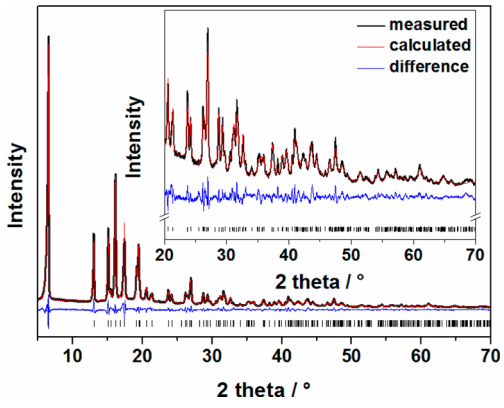

Figure 6. Final Rietveld plot of the structure refinement of $[Al_2(OH)_2(DPSTC)(H_2O)_2]\cdot 0.5H_2O$ (CAU-12). The observed powder pattern is shown in black, the calculated one is shown as an overlay in red, and the difference plot is shown in blue. The ticks mark the allowed Bragg peak positions. The inset shows the enlarged area of 20−70° (2θ).

oxygen atoms stem from the carboxylate groups of four linker molecules, and two are from bridging μ-OH groups. In the second type only two oxygen atoms stem from carboxylate groups of two linker molecules, two from the bridging μ-OH groups and two from coordinating water molecules (Figure 7, left). All of the Al−O distances range from 1.800(7) to 1.962(5) Å, which is in good agreement with the values of recently published Al-MOFs.[20,26] The structure achieves a three-dimensional framework through the connection of four inorganic chains with the carboxylate groups of the linker molecules (Figure 7, right). The linker molecules adopt a specific connection type since two of the four carboxylate groups are coordinated to two adjacent aluminum atoms in a bidentate bridging mode and the remaining two carboxylate groups are coordinated only to one aluminum atom in a monodentate manner (Figure 7, middle). The noncoordinating C−O bond is probably deprotonated, which is supported by the C2−O2 distance of 1.271(9) Å.[41] Furthermore, the IR spectrum does not contain a band around 1720−1700 cm^{-1}, which would be characteristic for the presence of −COOH groups. The noncoordinating oxygen atom of the $-CO_2$ group is in close contact to one coordinating water molecule of the neighboring AlO_6 octahedron suggesting possible hydrogen bonding (Figure 7, left). The sulfone group is distributed over two crystallographically equivalent positions which are each half occupied.

Structure Description of $[Al_2(OH)_2(DPSTC)]\cdot nH_2O$. The structure of CAU-12-dehy was refined from laboratory PXRD data. Using the structure of CAU-12, the structure model for CAU-12-dehy was set up by force-field calculations using the program Materials Studio.[40] The final Rietveld plot is shown in Figure 8.

The structure of CAU-12-dehy is closely related to that of CAU-12. It consists of the MIL-53 type inorganic building unit (Figure 9, left). The removal of the coordinated water molecules induce a rotation of the linker molecule (Figure 7, right, and Figure 9, middle), and the previously monodentate coordinating carboxylate groups now also bind via the second oxygen atom to adjacent Al atoms resulting in a bidentate coordination mode. The pores can be seen in Figure 9, right, where the view of the crystal structure along the *c*-axis is displayed.

DOI: 10.1021/ic502242j
Inorg. Chem. 2015, 54, 492−501

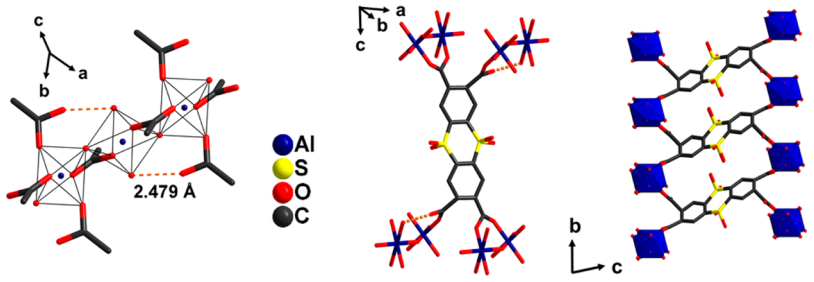

Figure 7. Structure of $[Al_2(OH)_2(DPSTC)(H_2O)_2]\cdot 0.5H_2O$ (CAU-12). Left: Inorganic building unit with two different types of AlO_6 octahedra. Middle: Coordination mode of one linker molecule. Right: View along the inorganic chains. Hydrogen bonds are shown as red dashed lines.

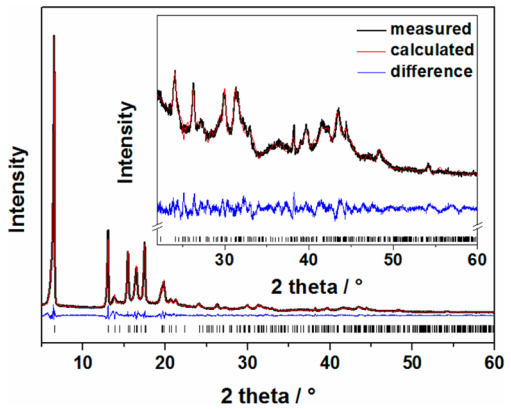

Figure 8. Final Rietveld plot of the structure refinement of $[Al_2(OH)_2(DPSTC)]\cdot nH_2O$. The observed powder pattern is shown in black, the calculated one is shown as an overlay in red, and the difference plot is shown in blue. The ticks mark the allowed Bragg peak positions. The inset shows the enlarged area of 22−60° (2θ).

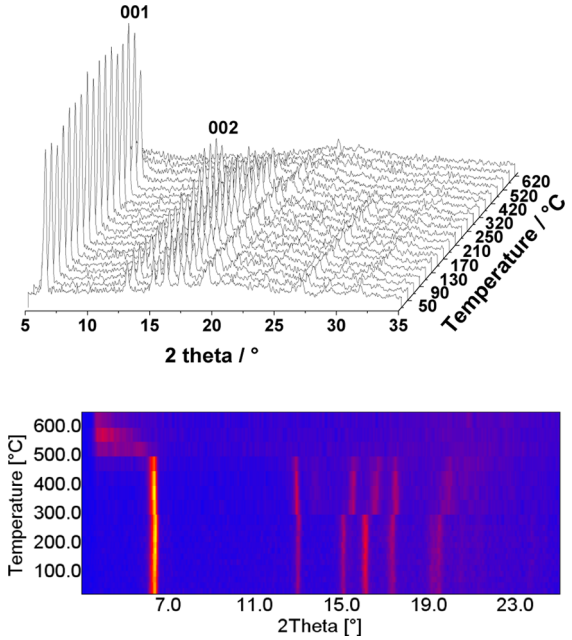

Figure 10. Top: TD-PXRD of CAU-12 in steps of 20 °C from 30 °C up to 270 °C and in steps of 50 °C from 270 °C up to 620 °C. Bottom: Top view corresponding to the TD-PXRD measurement of CAU-12.

Thermal Stability. All compounds were investigated concerning their thermal stability in air by thermogravimetric (TG) measurements (Supporting Information Figures S16, S19, and S22) and temperature dependent (TD) PXRD measurements (Figure 10 and Supporting Information Figures S17, S18, S20, and S21). The results of the TG measurements are summarized in Table 2.

The results obtained from the TG measurements for CAU-11 and CAU-11-COOH (Supporting Information Figures S16 and S19) are in good agreement with the deduced molecular formulas and reveal a high thermal stability for the two compounds. The thermal stability is additionally confirmed by TD-PXRD measurements (Supporting Information Figures S17 and S20).

The TG measurement of CAU-12 shows a two-step weight loss (Supporting Information Figure S22). From the molecular formula $[Al_2(OH)_2(DPSTC)(H_2O)_2]\cdot 0.5H_2O$ the first step (RT to 250 °C) can be attributed to the removal of coordinating and noncoordinating water molecules (measured 8.8%, calcd 8.6%) and the second (300−600 °C) to the decomposition of the framework (measrued 69.8%, calcd 71.9%) resulting in Al_2O_3 (measured 21.4%, calcd 19.5%). The TD-PXRD measurement (Figure 10, top) shows that the compound preserves its crystallinity up to 420 °C. As observed in the TG curve, the compound decomposes rapidly above 420 °C, and amorphous Al_2O_3 is formed. Above 270 °C a small shift of the first two reflections (001 and 002) toward lower diffraction angles is observed, and the remaining observable reflections shift to higher diffraction angles (Figure 10,

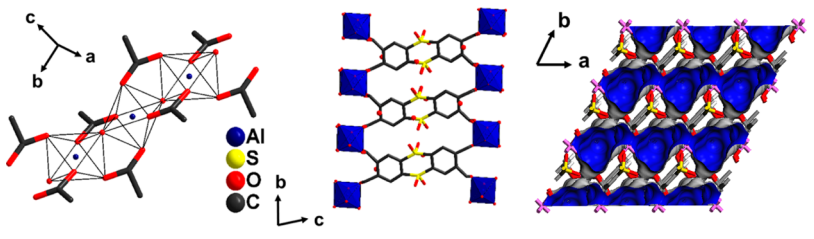

Figure 9. Structure of $[Al_2(OH)_2(DPSTC)]\cdot nH_2O$ (CAU-12-dehy). Left: Inorganic building unit, showing the full coordination of all carboxylate groups. Middle: View along the inorganic chains. Right: Connolly surface calculated with Materials Studio.[40]

DOI: 10.1021/ic502242j
Inorg. Chem. 2015, 54, 492−501

Table 2. Summary of the Results of the TG Measurements of CAU-11, CAU-11-COOH, and CAU-12

temp range/ °C	fragment	mass fraction % measured	mass fraction % calcd
CAU-11			
RT-425	0.25 DMF	5.3	5.0
425−600	framework	80.6	81.1
>600	Al_2O_3	14.1	13.9
CAU-11-COOH			
RT-280	0.5 H_2O	2.2	2.1
350−650	framework	86.0	85.8
>650	Al_2O_3	11.8	12.1
CAU-12			
RT-250	2.5 H_2O	8.8	8.6
300−600	framework	69.8	71.9
>600	Al_2O_3	21.4	19.5

bottom). In accordance with the TG measurement, the removal of the coordinating water molecules should be completed at this temperature (~270 °C), and therefore, the conversion into the dehydrated form of CAU-12 has taken place.

Vibrational Spectroscopy. IR spectra were collected of the as-synthesized CAU-11, a sample washed in DMF, and a sample activated at 200 °C after the sorption measurements. In all spectra a sharp ν_{OH}-band at 3581 cm^{-1} due to μ-OH groups in the framework can be observed (Supporting Information Figure S23). Also, the characteristic signals of the asymmetric and symmetric stretching vibration of the coordinating carboxylate groups are clearly visible at ν_{as} = 1630 and ν_s = 1433 cm^{-1}. The as-synthesized sample shows a small $\nu_{C=O}$-band at 1704 cm^{-1} indicating the presence of minor residues of unreacted acid. This band disappears, when the sample is treated with DMF, but the $\nu_{C=O}$-band of the DMF molecules emerges at 1684 cm^{-1}. Thus, DMF is adsorbed in the pores of CAU-11. After the activation of the sample and the subsequent sorption measurement vibrations in this region were no longer observed, indicating total removal of unreacted acid and DMF. In all spectra the preservation of the sulfone groups is indicated by the ν_{SO2}-bands at 1303 and 1148 cm^{-1} which are due to the asymmetric and symmetric stretching vibrations as well as the δ_{SO2}-vibration at 543 cm^{-1}.[42]

The IR spectra of CAU-11-COOH, CAU-12, and CAU-12-dehy are shown in (Figure 11). In the IR-spectrum of CAU-11-COOH a ν_{OH}-band at 3588 cm^{-1} is visible showing the presence of μ-OH groups within the framework (Figure 11, black). Next to the characteristic bands of the asymmetric and symmetric stretching vibrations at 1625, 1437, and 1407 cm^{-1} due to the coordinating carboxylate groups a $\nu_{C=O}$-band at 1732 cm^{-1} is observed indicating the presence of free carboxylic acid groups. Since this vibration did not change during the sample treatment with different solvents, these groups are assigned to be the noncoordinating −COOH groups. The vibrations of the SO_2 groups are present at ν_{SO2} = 1322 and 1144 cm^{-1} and δ_{SO2} = 555 cm^{-1}.[42]

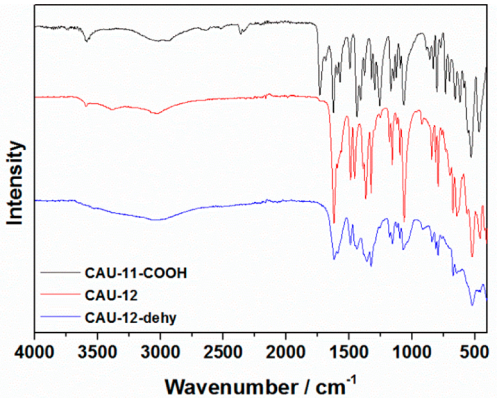

Figure 11. IR spectra of CAU-11-COOH (black), CAU-12 (red), and CAU-12-dehy (blue).

The IR-spectrum of CAU-12 also shows a small ν_{OH}-band at 3593 cm^{-1} due to μ-OH groups (Figure 11, red). The absence of a band around 1700 cm^{-1} indicates full deprotonation of the linker molecule and the presence of four $-COO^-$ groups in the product. The characteristic stretching vibrations of the carboxylate groups are observed at ν_{as} = 1620 cm^{-1} and ν_s = 1457 cm^{-1}, and also the vibrations of the SO_2 groups are present at ν_{SO2} = 1324 and 1156 cm^{-1} and δ_{SO2} = 561 cm^{-1}.[42] The IR spectrum of CAU-12-dehy exhibits broad overlapping bands at similar positions. Due to the adsorption of water from the atmosphere and the formation of hydrogen bonds, a very broad band from 2800−3600 cm^{-1} is observed.

Sorption Properties. To probe the sorption behavior of all compounds, measurements using different adsorptives were performed. Nitrogen as well as hydrogen sorption measurements were carried out at 77 K. Water vapor, carbon dioxide, as well as methane sorption measurements were performed at 298 K. Prior to each measurement, CAU-11 and CAU-11-COOH were activated at 200 °C (the total removal of DMF molecules from CAU-11 was verified by IR spectroscopy, Supporting Information Figure S23) and CAU-12 at 250 °C overnight under vacuum. In order to demonstrate the water stability of CAU-11 a second activation step using water (120 °C, 1 h, microwave irradiation) was carried out. No influence on the sorption properties was observed. The results of all measurements of all three samples are listed in Table 3.

Table 3. Results of the Sorption Measurements for CAU-11, CAU-11-COOH, and CAU-12 Using Various Adsorptives

	CAU-11	CAU-11-COOH	CAU-12-dehy
N_2 (a_{BET}, V_{mic}) (77 K)	350 m^2/g, 0.17 cm^3/g ($V_{mic,theor}$ = 0.18 cm^3/g)[43]		
H_2/wt % (77 K)	0.7	0.02	0.1
H_2O/wt % (298 K)	8.5	3.0	12.0
CO_2/wt % (298 K)	5.6	1.0	1.8
CH_4/wt % (298 K)	1.0		

The type I nitrogen isotherm of CAU-11 (Figure 12, top) demonstrates the microporosity of the compound. The specific surface area is about 350 m^2 g^{-1}, and the micropore volume is 0.17 cm^3 g^{-1} (p/p_0 = 0.5, theoretical volume calculated with Platon:[43] $V_{m(theor)}$ = 0.18 cm^3g^{-1}). Since the sulfone groups do not point into the pore channels but toward the inorganic chains, the water vapor isotherm is a type-III isotherm (Figure 12, bottom), showing the characteristic shape for a hydrophobic compound.

In Supporting Information Figure S24, sorption isotherms of the other gases are shown. At 100 kPa and 77 K, 0.7 wt % hydrogen is adsorbed, and 5.3 wt % of carbon dioxide is

DOI: 10.1021/ic502242j
Inorg. Chem. 2015, 54, 492−501

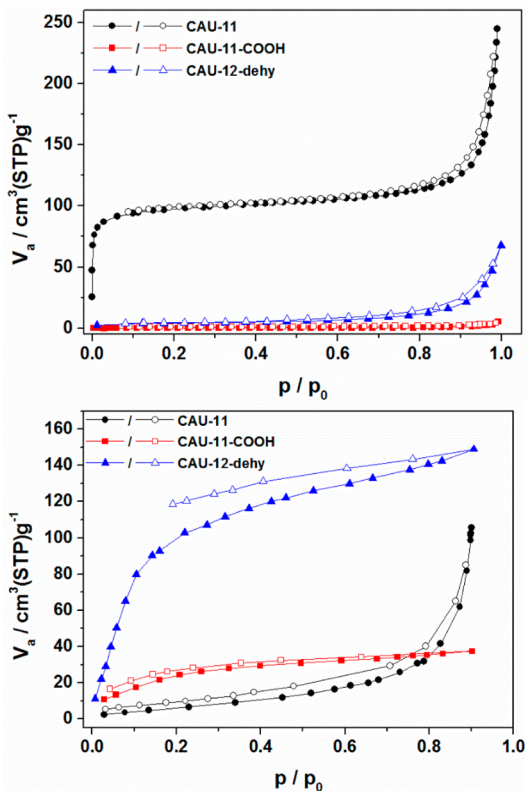

Figure 12. Results of the sorption measurements of CAU-11, CAU-11-COOH, and CAU-12-dehy. Top: Nitrogen gas sorption measurements (77 K). Bottom: Water vapor sorption measurements (298 K).

adsorbed at 100 kPa at 298 K. The uptake of 1.0 wt % of methane (100 kPa, 298 K) demonstrates the hydrophobic character of the compound.

Due to the additional carboxylic acid groups in the pores, CAU-11-COOH becomes nonporous toward nitrogen, but in contrast to CAU-11, uptake of H_2O is clearly observed at low p/p_0 values (Figure 12). The maximum uptake is only 3.0 wt %, but this is due to the small pores. The pore size and the hydrophilicity of the pores in CAU-11-COOH can also be used to explain the very low uptake of hydrogen, only 0.02 wt %, in contrast to a CO_2 uptake of 1.0 wt %, which has a bigger kinetic diameter but also a higher polarity than H_2, and can therefore be better adsorbed (see Supporting Information Figure S25).

CAU-12 shows a similar sorption behavior toward the adsorptives as observed for CAU-11-COOH. It is nonporous toward nitrogen, but it shows a strong affinity toward water vapor (uptake of 8.5 wt %), due to the incorporated and accessible sulfone groups (Figure 12). Accordingly, only a low uptake of 0.1 wt % of H_2 and yet a higher uptake of 1.8 wt % of CO_2 are observed, although H_2 has the smaller kinetic diameter but also lower polarity (see Supporting Information Figure S26).

CONCLUSION

In summary, we have discovered three new sulfone-functionalized Al-MOFs, using the high-throughput method. The syntheses were optimized, and the compounds were characterized in detail. The V-shape of the linker does not lead to the formation of a new inorganic building unit; instead, the very well-known inorganic building unit of trans corner-sharing AlO_6 polyhedra is observed. Interestingly, CAU-11 exhibits a layered structure, but nevertheless, it shows a high thermal stability up to 420 °C and a permanent porosity of 350 $cm^3\ g^{-1}$. This is due to 1D channels within the 2D layers resulting in an intralayer porosity. With this linker molecule, only very few porous compounds have been previously reported. In addition, the sorption properties can be altered by introducing additional noncoordinating carboxylic acid groups which turn the hydrophobic compound into the hydrophilic CAU-11-COOH. The third compound CAU-12 exhibits a three-dimensional network with a very uncommon coordination mode of the linker molecule and a high thermal stability up to 420 °C. During thermal activation, the compound transforms to its dehydrated form CAU-12-dehy. Coordinating water molecules are removed, and the free coordination site is filled by the noncoordinating part of the carboxylate groups. Such a structural conversion has only once been reported for an Al-MOF and underlines the high stability of such frameworks. The highly hydrophilic character of this compound due to the incorporated sulfone groups is proven by detailed sorption measurements.

ASSOCIATED CONTENT

Supporting Information

Reported compounds in the literature based on 4,4′-sulfonyldicarboxylic acid; exact compositions of the reaction mixtures in the high-throughput experiments and distributions of the different products; simulated structures of CAU-11-COOH; SEM picture of CAU-12; the asymmetric units and bond lengths; topology of CAU-11; TG curves of all compounds; IR spectra of CAU-11; TD-PXRD measurements of CAU-11 and CAU-11-COOH; H_2, CO_2, and CH_4 sorption measurements of CAU-11, CAU-11-COOH, and CAU-12-dehy. This material is available free of charge via the Internet at http://pubs.acs.org.

AUTHOR INFORMATION

Corresponding Author

*E-mail: stock@ac.uni-kiel.de.

Notes

The authors declare no competing financial interest.

ACKNOWLEDGMENTS

This work has been supported by the DFG (SPP 1362). The research leading to these results has received funding from the Europeans Community's Seventh Framework Program (FP7/2007-2013) under grant agreement 228862. A.K.I. is supported by the Knut and Alice Wallenberg Foundation through the MAX IV postdoctoral scholarship. We thank Milan Köppen for assistance with the Rietveld refinement of CAU-11.

REFERENCES

(1) Themed issue on Metal-Organic Framework: *Chem. Soc. Rev.* **2009**, *38*, 1201−1508.
(2) Themed issue on Metal-Organic Framework: *Chem. Rev.* **2012**, *112*, 673−1268.
(3) Themed issue on Metal-Organic Frameworks: *Chem. Soc. Rev.* **2014**, *43*, 5415−6172.
(4) Goesten, M. G.; Juan-Alcañiz, J.; Ramos-Fernandez, E. V.; Sai Sankar Gupta, K. B.; Stavitski, E.; van Bekkum, H.; Gascon, J.; Kapteijn, F. *J. Catal.* **2011**, *281*, 177−187.
(5) Horcajada, P.; Chalati, T.; Serre, C.; Gillet, B.; Sebrie, C.; Baati, T.; Eubank, J. F.; Heurtaux, D.; Clayette, P.; Kreuz, C.; Chang, J.-S.;

DOI: 10.1021/ic502242j
Inorg. Chem. 2015, 54, 492−501

Hwang, Y. K.; Marsaud, V.; Bories, P.-N.; Cynober, L.; Gil, S.; Férey, G.; Couvreur, P.; Gref, R. *Nat. Mater.* **2010**, *9*, 172−178.
(6) Couck, S.; Denayer, J. F. M.; Baron, G. V.; Remy, T.; Gascon, J.; Kapteijn, F. *J. Am. Chem. Soc.* **2009**, *131*, 6326.
(7) O'Keeffe, M. *Chem. Soc. Rev.* **2009**, *38*, 1215−1217.
(8) Reinsch, H.; Stock, N. *Microporous Mesoporous Mater.* **2013**, *171*, 156−165.
(9) Stock, N.; Biswas, S. *Chem. Rev.* **2012**, *112*, 933−969.
(10) Stock, N. *Microporous Mesoporous Mater.* **2010**, *129*, 287−295.
(11) Biswas, S.; Ahnfeldt, T.; Stock, N. *Inorg. Chem.* **2011**, *50*, 9518−9526.
(12) Reimer, N.; Gil, B.; Marszalek, B.; Stock, N. *CrystEngComm* **2012**, *14*, 4119−4125.
(13) Ahnfeldt, T.; Gunzelmann, D.; Wack, J.; Senker, J.; Stock, N. *CrystEngComm* **2012**, *14*, 4126−4136.
(14) Klinkebiel, A.; Reimer, N.; Lammert, M.; Stock, N.; Lüning, U. *Chem. Commun.* **2014**, *50*, 9306−9308.
(15) Ahnfeldt, T.; Gunzelmann, D.; Loiseau, T.; Hirsemann, D.; Senker, J.; Férey, G.; Stock, N. *Inorg. Chem.* **2009**, *48*, 3057−3064.
(16) Gaab, M.; Trukhan, N.; Maurer, S.; Gummaraju, R.; Müller, U. *Microporous Mesoporous Mater.* **2012**, *157*, 131−136.
(17) Loiseau, T.; Serre, C.; Huguenard, C.; Fink, G.; Taulelle, F.; Henry, M.; Bataille, T.; Férey, G. *Chem.—Eur. J.* **2004**, *10*, 1373−1382.
(18) Comotti, A.; Bracco, S.; Sozzani, P.; Horike, S.; Matsuda, R.; Chen, J.; Takata, M.; Kubota, Y.; Kitagawa, S. *J. Am. Chem. Soc.* **2008**, *130*, 13664−13672.
(19) Loiseau, T.; Mellot-Draznieks, C.; Muguerra, H.; Férey, G.; Haouas, M.; Taulelle, F. *C. R. Chim.* **2005**, *8*, 765−772.
(20) Niekiel, F.; Ackermann, M.; Guerrier, P.; Rothkirch, A.; Stock, N. *Inorg. Chem.* **2013**, *52*, 8699−8705.
(21) Senkovska, I.; Hoffmann, F.; Fröba, M.; Getzschmann, J.; Böhlmann, W.; Kaskel, S. *Microporous Mesoporous Mater.* **2009**, *122*, 93−98.
(22) Volkringer, C.; Loiseau, T.; Guillou, N.; Férey, G.; Haouas, M.; Taulelle, F.; Elkaim, E.; Stock, N. *Inorg. Chem.* **2010**, *49*, 9852−9862.
(23) Reinsch, H.; Krüger, M.; Wack, J.; Senker, J.; Salles, F.; Maurin, G.; Stock, N. *Microporous Mesoporous Mater.* **2012**, *157*, 50−55.
(24) Reinsch, H.; Marszalek, B.; Wack, J.; Senker, J.; Gil, B.; Stock, N. *Chem. Commun.* **2012**, *48*, 9486−9488.
(25) Reinsch, H.; van der Veen, M. A.; Gil, B.; Marszalek, B.; Verbiest, T.; de Vos, D.; Stock, N. *Chem. Mater.* **2013**, *25*, 17−26.
(26) Reinsch, H.; Krüger, M.; Marrot, J.; Stock, N. *Inorg. Chem.* **2013**, *52*, 1854−1859.
(27) Reinsch, H.; De Vos, D.; Stock, N. *Z. Anorg. Allg. Chem.* **2013**, *639*, 2785−2789.
(28) Gándara, F.; Andrés, A. d.; Gómez-Lor, B.; Gutiérrez-Puebla, E.; Iglesias, M.; Monge, M. A.; Proserpio, D. M.; Snejko, N. *Cryst. Growth Des.* **2008**, *8*, 378−380.
(29) Harbuzaru, B. V.; Corma, A.; Rey, F.; Atienzar, P.; Jordá, J. L.; García, H.; Ananias, D.; Carlos, L. D.; Rocha, J. *Angew. Chem.* **2008**, *120*, 1096−1099.
(30) Gándara, F.; Gomez-Lor, B.; Gutiérrez-Puebla, E.; Iglesias, M.; Monge, M. A.; Proserpio, D. M.; Snejko, N. *Chem. Mater.* **2008**, *20*, 72−76.
(31) Zhuang, W.-J.; Zheng, X.-J.; Sun, H.-L.; Jin, L.-P.; Xuebao, W. H. *Chin. J. Struct. Chem.* **2008**, *24*, 1305−1310.
(32) Li, H.; Shi, W.; Zhao, K.; Niu, Z.; Chen, X.; Cheng, P. *Chem.—Eur. J.* **2012**, *18*, 5715−5723.
(33) Yeh, C.-T.; Lin, W.-C.; Lo, S.-H.; Kao, C.-C.; Lin, C.-H.; Yang, C.-C. *CrystEngComm* **2012**, *14*, 1219−1222.
(34) Plonka, A. M.; Banerjee, D.; Woerner, W. R.; Zhang, Z.; Nijem, N.; Chabal, Y. J.; Li, J.; Parise, J. B. *Angew. Chem.* **2013**, *125*, 1736−1739.
(35) Wu, C.-Y.; Raja, D. S.; Yang, C.-C.; Yeh, C.-T.; Chen, Y.-R.; Li, C.-Y.; Ko, B.-T.; Lin, C.-H. *CrystEngComm* **2014**, *16*, 9308−9319.
(36) Willmott, P. R.; Meister, D.; Leake, S. J.; Lange, M.; Bergamaschi, A.; Boge, M.; Calvi, M.; Cancellieri, C.; Casati, N.; Cervellino, A.; Chen, Q.; David, C.; Flechsig, U.; Gozzo, F.; Henrich, B.; Jaggi-Spielmann, S.; Jakob, B.; Kalichava, I.; Karvinen, P.; Krempasky, J.; Ludeke, A.; Luscher, R.; Maag, S.; Quitmann, C.; Reinle-Schmitt, M. L.; Schmidt, T.; Schmitt, B.; Streun, A.; Vartiainen, I.; Vitins, M.; Wang, X.; Wullschleger, R. *J. Synchrotron Radiat.* **2013**, *20*, 667−682.
(37) Favre-Nicolin, V.; Cerny, R. *J. Appl. Crystallogr.* **2002**, *35*, 734−743.
(38) Barthelet, K.; Riou, D.; Nogues, M.; Férey, G. *Inorg. Chem.* **2003**, *42*, 1739−1743.
(39) *Topas Academics v4.1*; Coelho Software: Brisbane, Australia, 2007.
(40) *Materials Studio Version 5.0*; Accelrys Inc.: San Diego, CA, 2009.
(41) Volkringer, C.; Loiseau, T.; Guillou, N.; Ferey, G.; Haouas, M.; Taulelle, F.; Audebrand, N.; Margiolaki, I.; Popov, D.; Burghammer, M.; Riekel, C. *Cryst. Growth Des.* **2009**, *9*, 2927−2936.
(42) Socrates, G. *Infrared and Raman Characteristic Group Frequencies:* Tables and Charts, 3*rd ed.*; Wiley, 2004.
(43) Spek, A. L. P., Multipurpose, A.; Crystallographic Tool v 1.16, Utrecht Universität: Utrecht, Niederlande, 2011.

DOI: 10.1021/ic502242j
Inorg. Chem. 2015, 54, 492−501